

Contrasting ring-opening propensities in UV-excited α -pyrone and coumarin

Daniel Murdock,¹ Rebecca A. Ingle,¹ Igor Sazanovich,² Ian P. Clark,² Yu Harabuchi,³ Tetsuya Taketsugu,³ Satoshi Maeda,³ Andrew J. Orr-Ewing,¹ and Michael N. R. Ashfold¹

¹School of Chemistry, University of Bristol, Cantock's Close, Bristol, BS8 1TS, United Kingdom

²Central Laser Facility, Research Complex at Harwell, Science and Technologies Facilities Council, Rutherford Appleton Laboratory, Didcot, Oxfordshire, OX11 0QX, United Kingdom

³Department of Chemistry, Faculty of Science, Hokkaido University, Sapporo 060-0810, Japan

Supporting Information

A. Steady-state UV absorption spectra

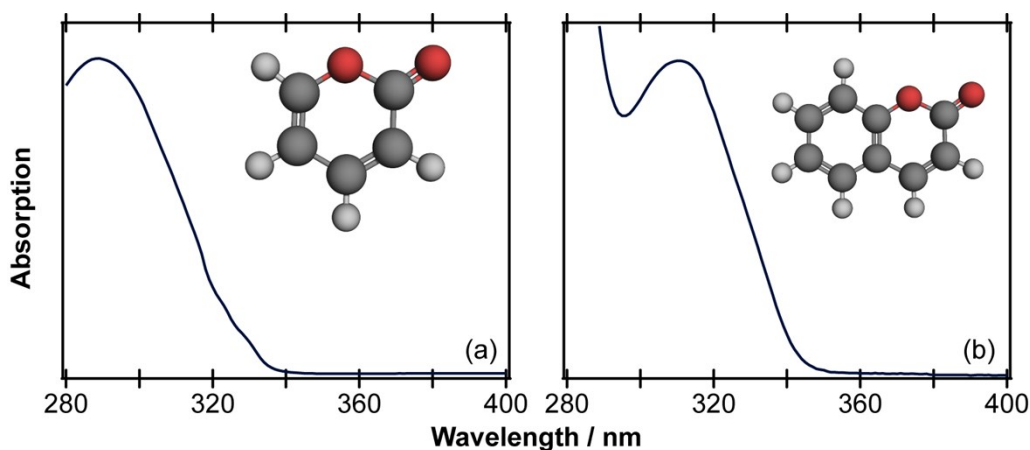


Figure S1. UV absorption spectra of (a) α -pyrone and (b) coumarin.

B. Spectral decomposition

i. α -pyrone carbonyl stretch region

The parent bleach was modeled as the sum of five Gaussian-type features:

$$y(x) = P \sum_n A_n \exp \left\{ - \left(\frac{x - x_n}{w_n} \right)^2 \right\}$$

with the peak centers (x_n), widths (w_n), and relative amplitudes (A_n) obtained from a simultaneous fit to all the available data. The overall amplitude (P) was allowed to float (while the ratios between the individual Gaussians remained fixed) for the fit to each individual time-slice, with this parameter providing a measure of the parent molecule population. The photoproduct carbonyl peaks were modeled as the sum of three Gaussian functions.

The vibrationally hot α -pyrone (S_0) signal was modeled using three Gaussian functions (v1, v2, and v3 in figure S2), whose peak centres and widths were fixed to the best-fit value obtained from a simultaneous fit to all available data. The individual amplitudes were allowed to float for each time slice.

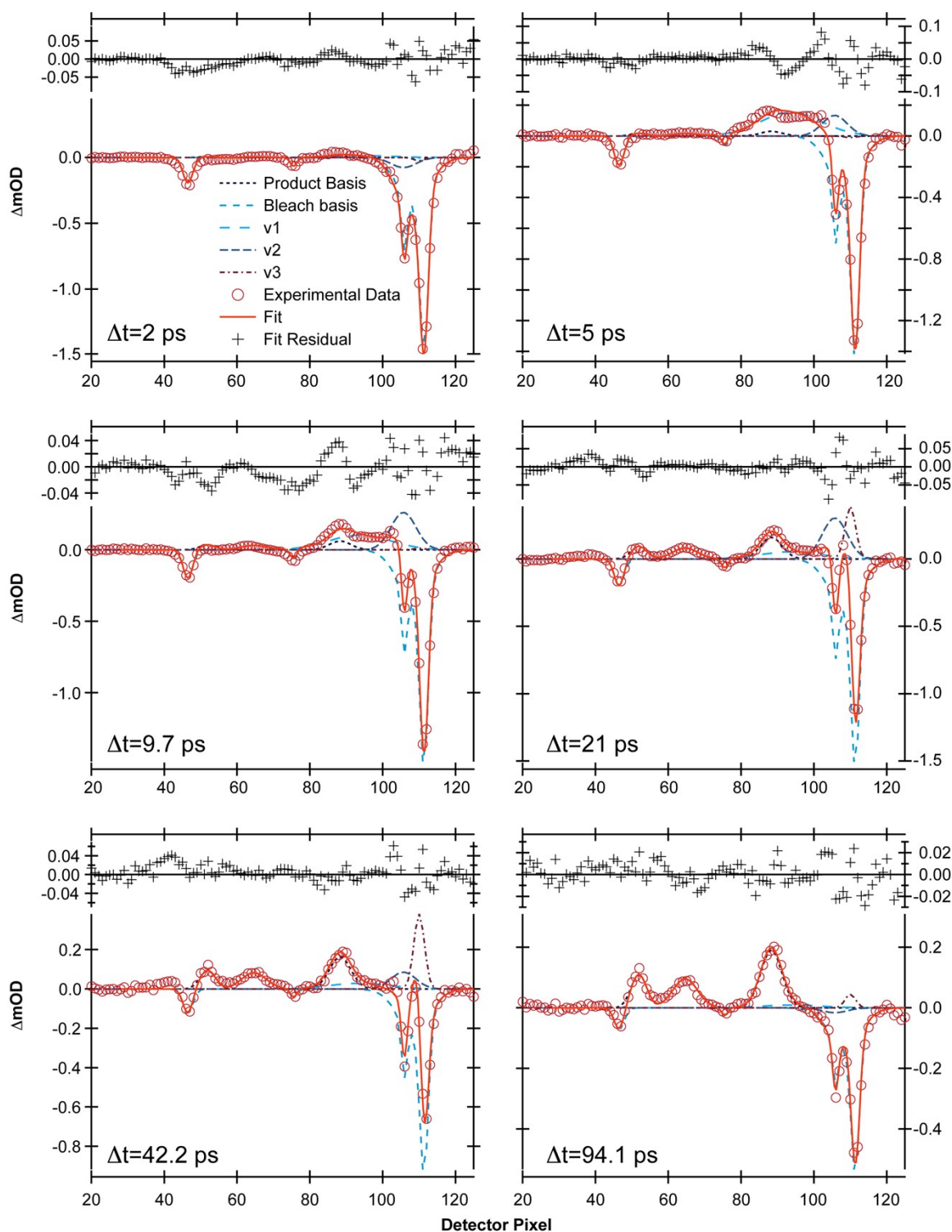


Figure S2. Decomposition of a series of 310 nm pump, carbonyl probe, TVA spectra of α -pyrone in terms of model functions.

ii. α -pyrone ketene stretch region

At early times ($\Delta t < 35$ ps; figure S3), the ketene feature was fit as the sum of two shifted but otherwise identical Lorentzian-type functions:

$$y(x) = A \left(\frac{1}{(x - x_n)^2 + B} + \frac{1}{(x - (x_n + dx))^2 + B} \right)$$

where the amplitude (A), width (B), and peak centre (x_n) were allowed to float in the fit to each time slice. The spacing between the two Lorentzians (dx) was determined by a simultaneous fit to all data.

For the later time data ($\Delta t > 35$ ps; figure S4) the ketene feature was again modeled as the sum of two Lorentzians. The width, peak centre, and spacing between the peaks were obtained by simultaneously fitting all the data. The amplitudes of the two Lorentzians were allowed to float separately, thus providing a measure of isomer population as a function of pump/probe delay time.

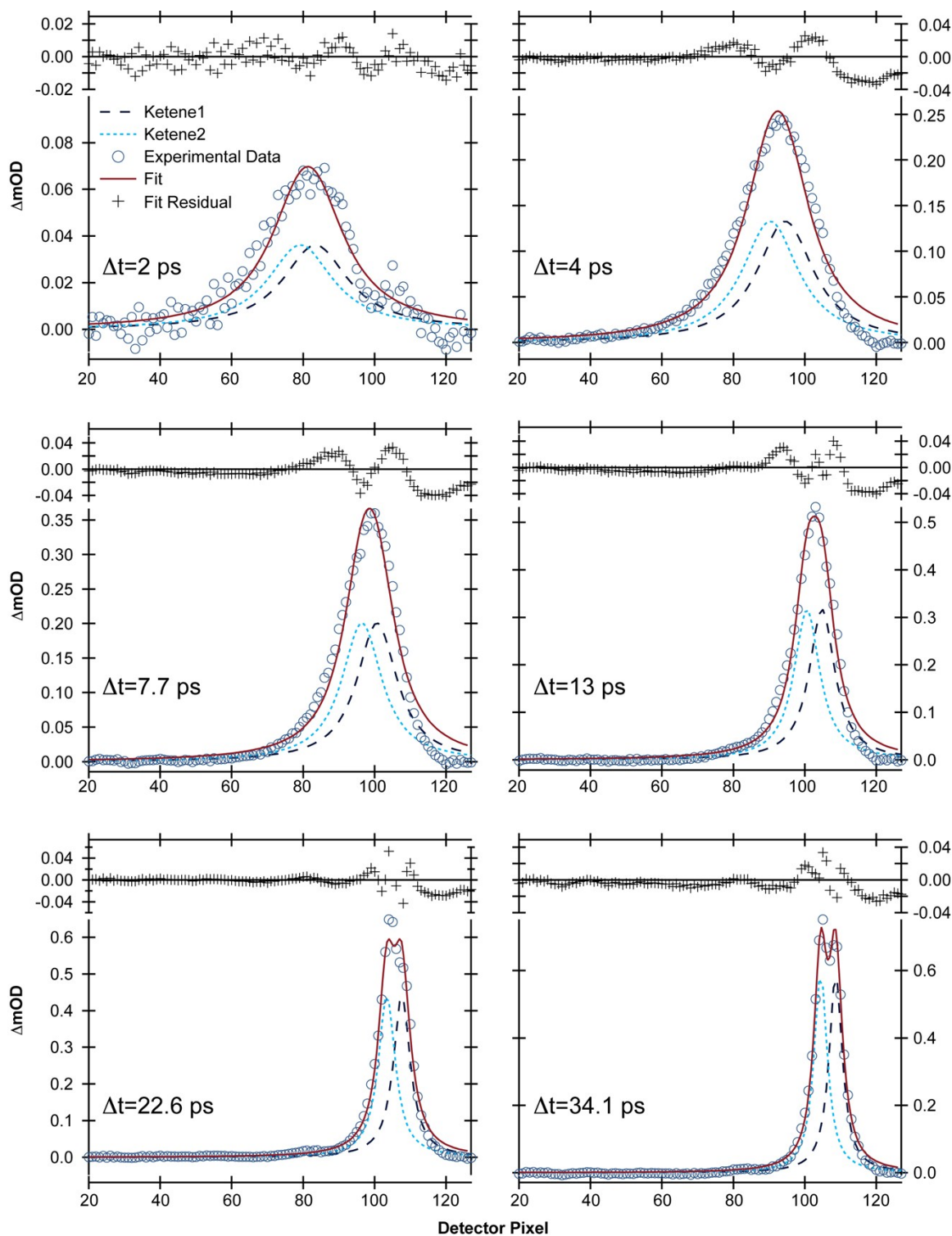


Figure S3. Decomposition of a series of 310 nm pump, ketene probe, TVA spectra of α -pyrone for time delays $\Delta t < 35$ ps in terms of the model functions described in the text.

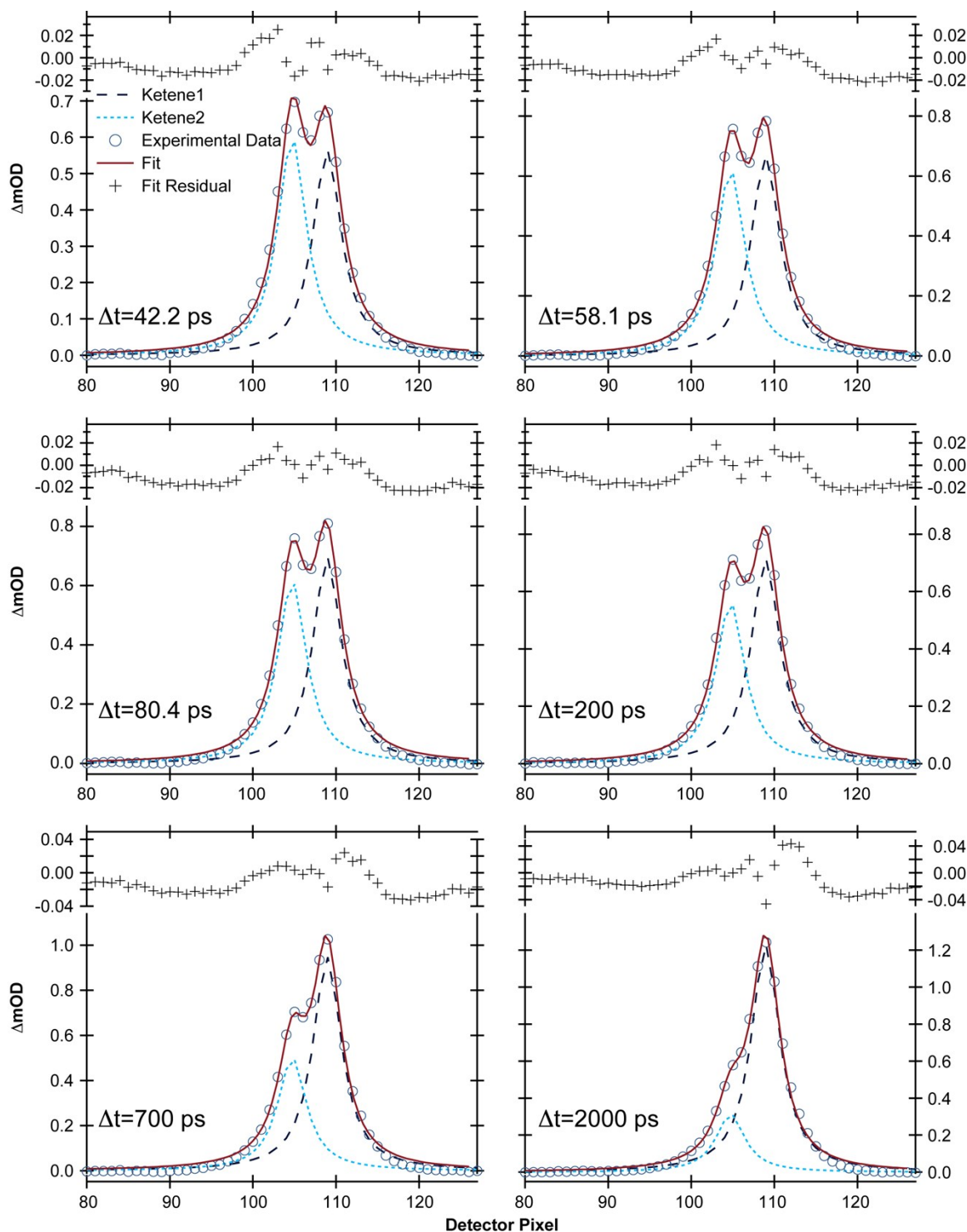


Figure S4. Decomposition of a series of 310 nm pump, ketene probe, TVA spectra of α -pyrone for time delays $\Delta t \geq 35$ ps in terms of the model functions described in the text.

iii. Coumarin carbonyl stretch region

The parent bleach was modeled as the sum of four Gaussian-type features with the peak centers (x_n), widths (w_n), and relative amplitudes (A_n) obtained from a simultaneous fit to all the available data. The overall amplitude (P) was allowed to float for the fit to each individual time-slice, with this parameter providing a measure of the parent molecule population.

The vibrationally hot coumarin signal was modeled using two Gaussian functions (v1 and v2 in figure S5). The width of v1 was fixed to be 10 pixels, and the peak was centered around pixel number 5 on the detector. The amplitude was allowed to float. All fit parameters describing v2 were allowed to float for each time slice.

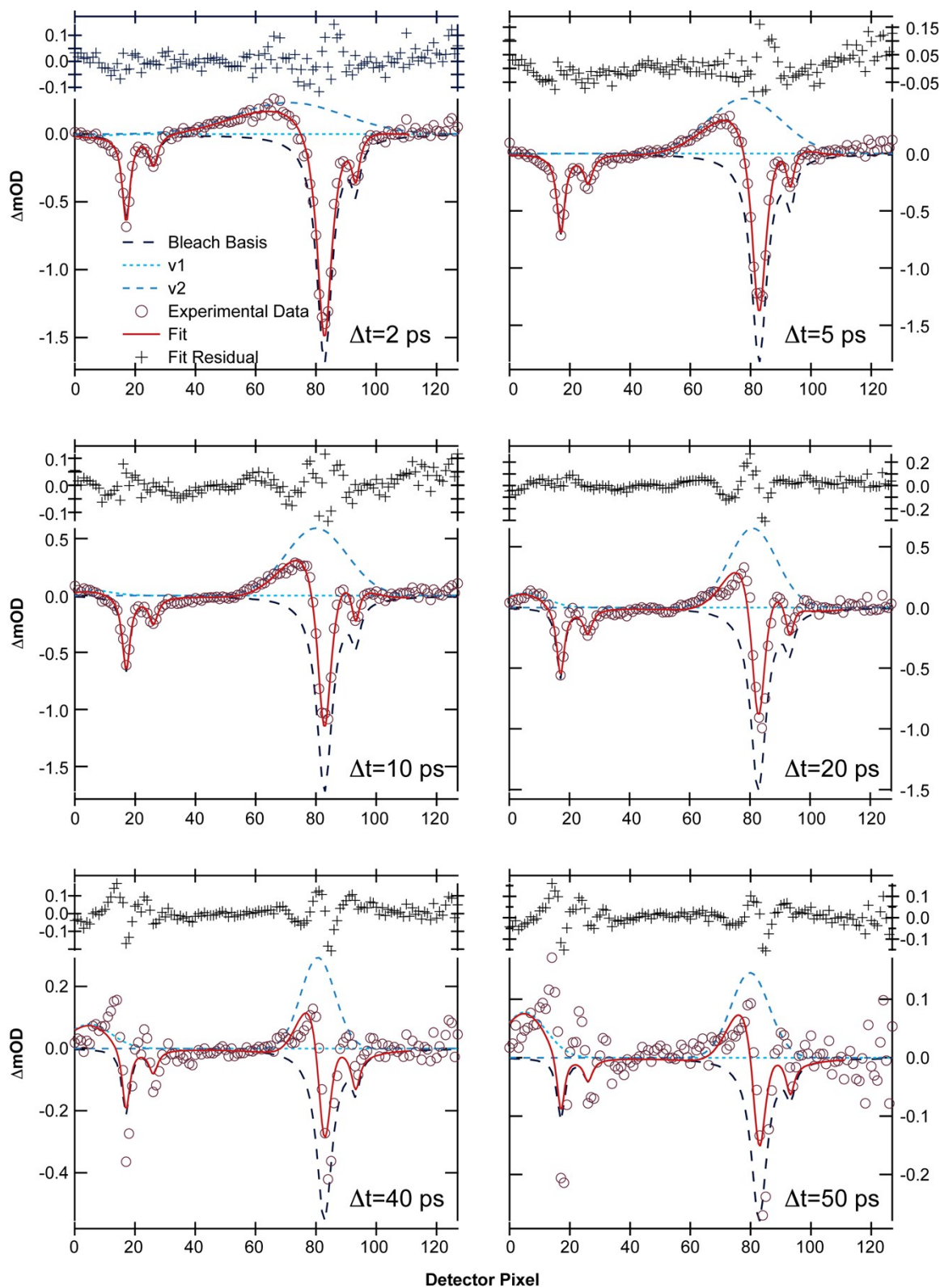
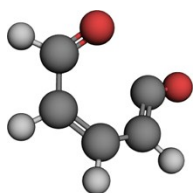


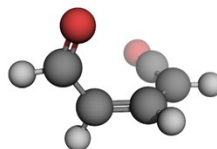
Figure S5. Decomposition of a series of 330 nm pump TVA spectra of coumarin in terms of the model functions described in the text.

C. Minimum energy conical intersections of α -pyrone



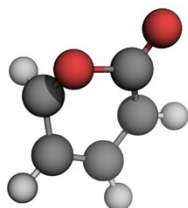
MECI-1
 $\Delta E = 3.94$ eV

C	0.97746	0.24543	-1.14915
C	-0.33844	0.34858	-1.42007
C	1.61976	0.12699	0.11418
H	-0.67295	0.50898	-2.43746
H	2.6031	-0.31792	0.12146
C	-1.38593	0.16487	-0.40276
C	1.19184	0.71015	1.37937
H	1.82872	0.43876	2.23175
H	1.64212	0.22677	-2.00209
O	0.26757	1.4706	1.52484
O	-2.54845	0.14664	-0.58965



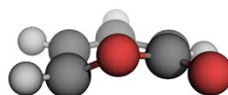
MECI-2
 $\Delta E = 4.00$ eV

C	-0.18625	0.14866	-1.70846
C	0.98096	0.46048	-1.13676
C	1.34943	0.01686	0.14749
C	0.52487	-0.87263	0.94402
C	-0.47715	-0.40403	1.82202
O	-0.75769	0.78381	1.98071
O	-1.17829	-0.11196	-2.23118
H	1.61692	1.10897	-1.71795
H	2.28152	0.38981	0.5446
H	0.68506	-1.94168	0.88735
H	-1.02222	-1.17688	2.37652



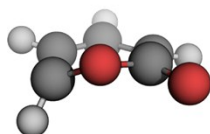
MECI-3
 $\Delta E = 4.15$ eV

C	1.29085	0.14462	-1.15189
C	-0.12775	-0.08698	-1.10875
C	1.904	0.35572	0.02423
H	-0.66959	-0.38134	-1.98994
H	2.88818	0.76818	0.16888
C	-0.94303	0.3833	-0.03797
C	0.93832	0.06854	1.08903
H	0.93849	-0.83722	1.68069
H	1.7947	0.21219	-2.10487
O	-0.12879	0.82512	1.13435
O	-2.12068	0.44583	0.08527



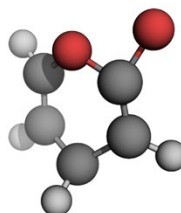
MECI-4
 $\Delta E = 5.06$ eV

C	1.22741	0.46845	-1.11449
C	-0.25693	0.27006	-1.2529
C	1.78436	0.33999	0.07347
H	-0.82904	0.65709	-2.0726
H	2.84712	0.41668	0.23481
C	-0.76508	-0.3863	-0.26016
C	0.91524	-0.00815	1.21961
H	1.30222	-0.35351	2.16019
H	1.80914	0.65197	-2.00216
O	-0.1642	-0.82123	0.84985
O	-2.02253	-0.77317	0.21175



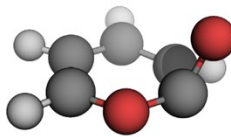
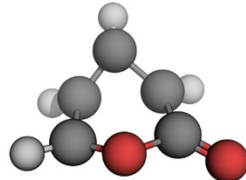
MECI-5
 $\Delta E = 5.13$ eV

C	1.28446	-0.0695	-1.17708
C	-0.19333	0.16817	-1.26129
C	1.85077	-0.19729	0.0056
H	-0.67637	0.55296	-2.1377
H	2.88733	-0.4636	0.13484
C	-0.8256	-0.15088	-0.1767
C	0.98721	-0.12643	1.20625
H	1.07833	0.57491	2.01869
H	1.83684	-0.21108	-2.09155
O	-0.31773	-0.57372	1.00179
O	-2.11086	-0.08194	0.3331



MECI-6
 $\Delta E = 5.29$ eV

C	1.33608	-0.47629	-1.29622
C	-0.179	-0.57446	-1.3192
C	1.86108	-0.44496	0.06277
H	-0.70713	-1.18227	-2.03032
H	2.87497	-0.73622	0.28987
C	-0.74744	-0.04662	-0.28958
C	1.09651	-0.01371	1.05972
H	1.34566	0.06913	2.09964
H	1.84219	0.11847	-2.04383
O	-0.17187	0.49491	0.79905
O	-2.00245	-0.02674	0.3311

							
MECI-7 $\Delta E=5.30$ eV				MECI-8 $\Delta E=5.31$ eV			
C	1.02322	0.04822	-1.15811	C	1.15011	-0.99665	-1.1128
C	-0.2646	0.64616	-1.16563	C	0.03344	-0.04981	-1.06825
C	1.62536	-0.07784	0.08415	C	1.68868	-0.28218	-0.06383
H	-0.71542	1.03607	-2.05912	H	-0.17012	0.55885	-1.93234
H	2.63495	-0.4397	0.18069	H	2.67362	0.1757	-0.09953
C	-0.96929	0.79822	0.06843	C	-0.88916	0.05472	0.02502
C	0.96818	0.28197	1.2434	C	1.0158	-0.2796	1.24364
H	1.44099	0.28439	2.20968	H	1.50388	-0.64439	2.12931
H	1.51013	-0.26601	-2.06419	H	1.67746	-1.22177	-2.02151
O	-0.29358	0.67544	1.28882	O	-0.30694	-0.35516	1.23377
O	-1.64735	-0.2197	-0.38647	O	-2.00596	0.47704	0.03929

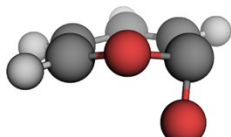
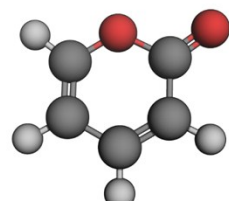
							
MECI-9 $\Delta E=6.36$ eV				S1-FC $\Delta E=5.05$ eV			
C	0.85299	1.16265	-1.22157	C	1.16606	4.11E-05	-1.19942
C	-0.26169	0.45146	-1.38638	C	-0.17639	-1.09E-04	-1.27168
C	1.29963	1.50343	0.12287	C	1.82138	-2.62E-05	0.0736
H	-0.63022	0.18982	-2.36438	H	-0.71172	2.29E-05	-2.20386
H	2.10319	2.20361	0.2699	H	2.89208	-1.03E-05	0.16216
C	-1.00603	-0.06873	-0.22468	C	-0.99124	1.98E-04	-0.0732
C	0.71107	0.96237	1.18268	C	1.04965	5.08E-06	1.16569
H	0.94288	1.15807	2.21289	H	1.41115	3.45E-06	2.17857
H	1.4332	1.5004	-2.06429	H	1.75771	1.28E-06	-2.1007
O	-0.26405	0.0103	1.04786	O	-0.28569	-5.07E-05	1.11601
O	-1.84407	0.71109	0.50824	O	-2.18418	-6.93E-05	-0.01775

Figure S6. Minimum energy conical intersections for α -pyrone obtained at the SF-BHLYP/6-31G(*d*) level of theory. The energies of each MECI relative to α -pyrone (S_0) are shown, along with the atomic coordinates (xyz format) relative to the centre-of-mass, in Å. MECI-1 is the 35° structure discussed in the main text, and MECI-2 is the 90° structure. Also included is the structure of α -pyrone (S_0) along with its vertical excitation energy to the S_1 state (S_1 -FC).

D. Coumarin ring-open isomers

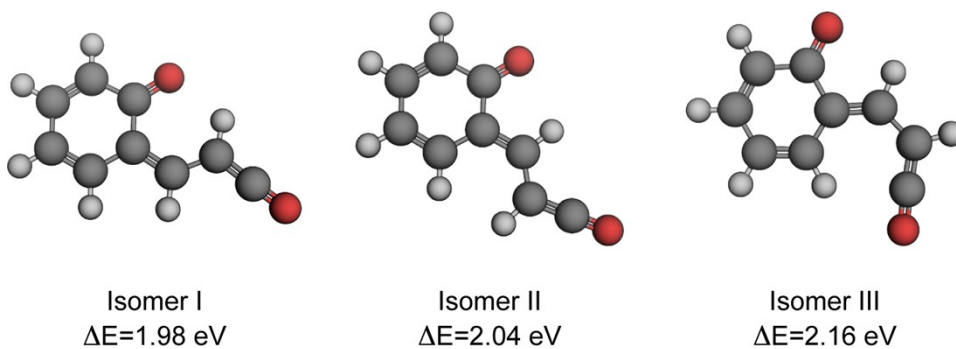


Figure S7. Stable ring-open isomers of coumarin calculated at the MP2/cc-pVTZ level of theory with implicit solvation by CH₃CN accounted for using the PCM method. All energies are quoted relative to the S₀ equilibrium value of the parent molecule.

E. Simulated IR spectra of ring-opened Z-isomers

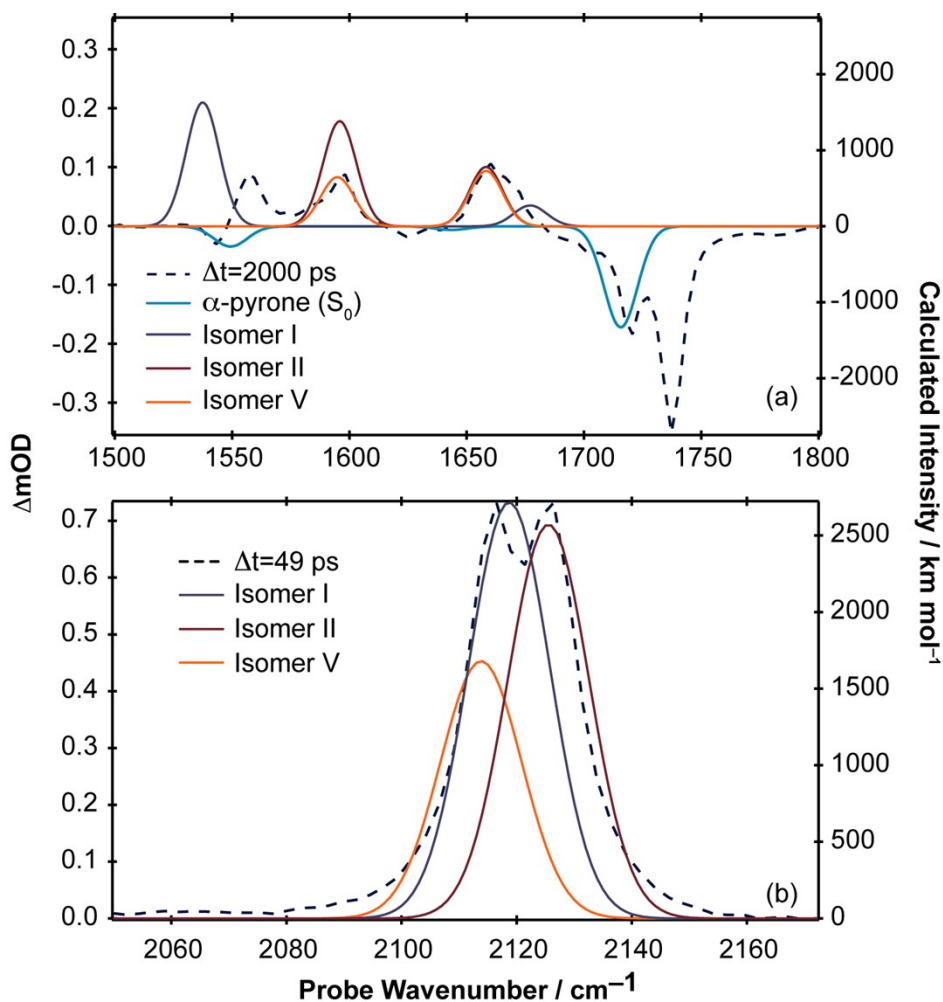


Figure S8. Simulated IR spectra for the three ring-open Z-isomers of α -pyrone calculated at the B3LYP/6-311++G(*d,p*) level of theory with implicit solvation accounted for using the PCM method. Panels (a) and (b) cover the 1500-1800 cm⁻¹ and 2050-2150 cm⁻¹ regions, respectively. The solid lines are the computed spectra (represented by Gaussian functions with 10 cm⁻¹ FWHM), and the dashed lines are the experimental data recorded at time delays of 2000 ps and 49 ps in (a) and (b), respectively. The calculated wavenumbers have been multiplied by 0.99 in (a), and 0.975 in (b).